Analysis of Structure and Movement of Neural Growth Cone

Fumiaki Nagase

Master's thesis
2013:E67

Lund University

Faculty of Engineering
Centre for Mathematical Sciences
Mathematics

Centrum Scientiarum Mathematicarum

Analysis of structure and movement of neural growth cone

Fumiaki Nagase

1. Janurary, 2014

Abstract

Growth cone is a sensory and motile part at the tip of a neuron and its main function is path finding. In previous works many chemical cascades and simple structure of growth cone were revealed. However, to understand the whole function of growth cone, deeper research on structure, especially on filopodia, is desired. Here, in this thesis, we developed a new method to segment growth cone and also count and categorize filopodia. Furthermore, evaluation of previous method and this new method were also established. By using this new software, deeper and more detailed research of structure of growth cone is now possible. The method has been tested on real data and evaluated against manually annotated ground truth with promising results.

.

Contents

.

1 Introduction

Axon growth directed by growth cone plays an important role during neural circuit formation. Growth cone is a sensory and motile part at the tip of a neuron and its main function is path finding. It receives chemical guidance molecules from circumstance via specific receptors. Many attractive and repulsive guidance cues and following cascades inside growth cone have been revealed by previous reports. These cascades lead to structural changing and growth cone's movements. Thus, to understand the whole mechanism of growth cone's function, both chemical and structural understandings of growth cone are needed. However, structural change of growth cone (corresponding to guidance cues) has not deeply clarified. At the previous report [1] it was already possible to obtain a rough analysis of images and shapes, however there was no evaluation or detail analysis of growth cone's feature such as filopodia. The analysis was limited in this report because only threshold method was used. Therefore, in this thesis, we developed software to analyze structure of growth cone more into detail with graph cuts method and scale-space method. The main target structure to research is filopodia.

In this thesis, basic structure of growth cone is firstly described. Then description of data set and methods follow. There are then results obtained by this new software and a short discussion and conclusion of this thesis.

1.1 Aim of the thesis

The aim of this thesis is to develop an algorithm for the analysis of the structure and movement of growth cone quantitatively and automatically. This software will be also used for the further work in outgrowth and guidance research of neural growth cone in the future.

2 Background

2.1 Basics of growth cone's structure

The main components of the structure of neuron and growth cone are actin and microtubule. There are some different definition of parts in growth cone however it is often divided into 3 parts, central domain (C-domain), transition zone (T zone) and peripheral domain (P-domain) (Figure 1) [5]. Axon is mainly constructed with microtubule and microtubules extend to growth cone C-domain. P-domain contains filopodium and lamellipodia which are constructed by actin. Filopodium is a bundle of actin and lamellipodia are mesh-polymerized actin. Motility of P-domain is really high and this part plays the main role on guidance cue receiving and direction decision.

3 Data

Cell culture and acquisition of images were carried out in Japan previously.

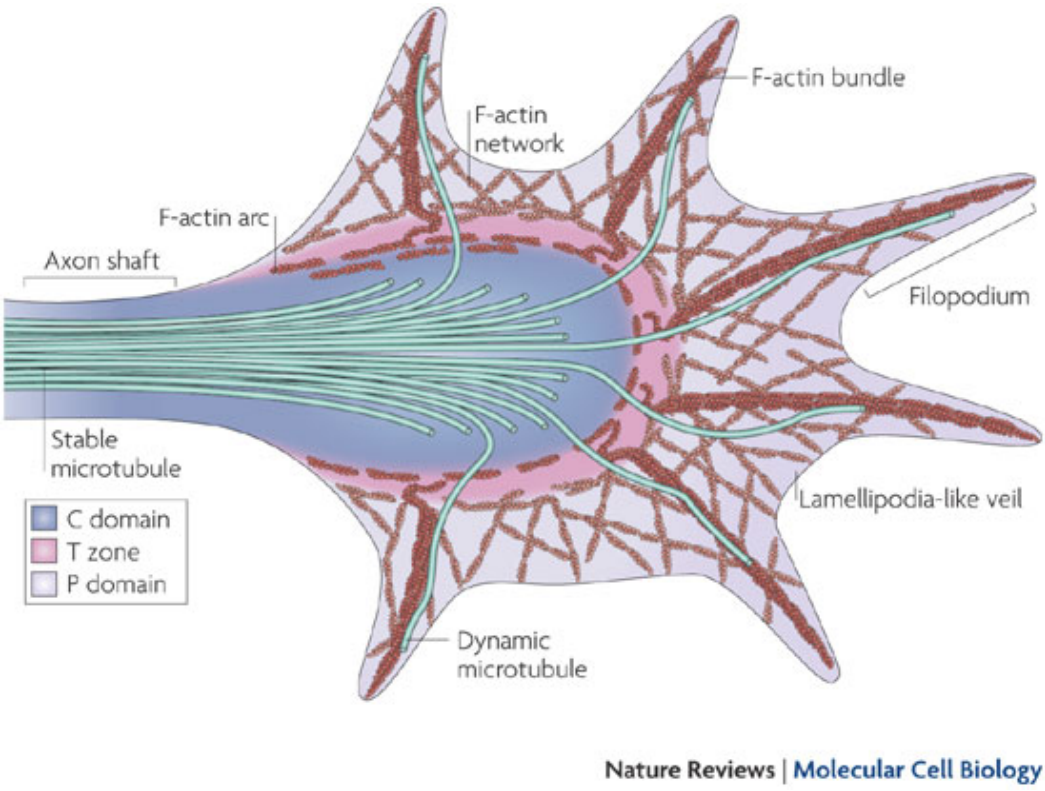

Figure 1: Structure of growth cone

3.1 Cell culture

Primary DRG neurons dissected from E18 rats (Charles River) were dissociated with 1 mg/mL trypsin (Sigma-Aldrich) in phosphate-buffered saline. All animal procedures were approved by the Ethics Committee of Keio University (permit number, 09106-(1)). The dissociated cells were resuspended in Neurobasal medium without phenol red (Life Technologies) supplemented with 2% B27 (Life Technologies) and 50 ng/mL nerve growth factor (Alomone Labs). The cells were transfected with plasmids coding FRET sensors such as Epac1-camps, red cGES-DE5 or YC 3.60 by electroporation using Neon (Life Technologies). The cells were plated on a dish coated with 0.01 mg/mL poly-D-lysine (Life Technologies). The cells were used after a minimum of 24 h in culture.

3.2 Acquisition of Image

Images are acquired by a laser scanning confocal microscope system (Olympus) mounted on an inverted microscope (Olympus) with a $\times 100$ oil immersion objective. Both donors of the FRET sensors were simultaneously excited using a diode laser at 405 nm, and the excitation was split using a beam splitter 20/80, the emission was split using 3 dichroic mirrors (490, 510, and 560 nm), and the emissions were acquired using 2 grating-based detectors (460-490 nm and 490-510 nm) and 2 filter based detectors (535-565 nm and 560-660 nm). Neurons were maintained at 37 °C in a humidified atmosphere of 5%CO_2 (Tokai Hit). One example of an original image before any image processing is shown in Figure 2.

3.3 Ground truth

The ground truth of a cell structure was constructed manually and the number of filopodia in each partition was also counted manually. To make a ground truth cell mask, a short MATLAB code was written. Built function, roipoly was used to obtain the cell structure by pointing the node of ROI of cell mask. Example of ground truth is shown in Figure 3.

4 Methods

4.1 Summary of Image processing

Images were analyzed using original image processing and analysis software written in MATLAB (MathWorks). The software is based on STAMI 2012 made in previous work [1]. To obtain fluorescence signal of each region, the images were processed as described (Figure 4). The parts written red were developed in this thesis. The goal of image process is to obtain real fluorescent signal and structure details such as number, slant and partition of filopodia.

4.2 Choice of methods used in this program

There are several possible method can be applied in this program, however in the following sections 2, the main methods used here are described. The other choice is, for instance, the fast marching method [6]. This method makes it

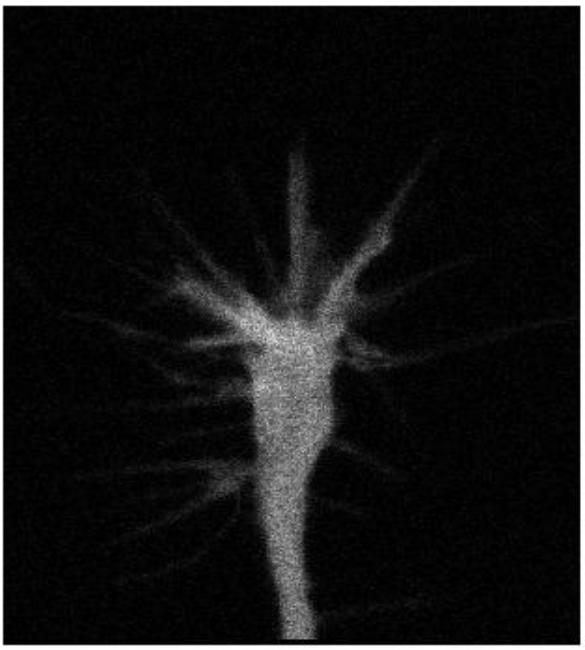

Figure 2: An original image of growth cone

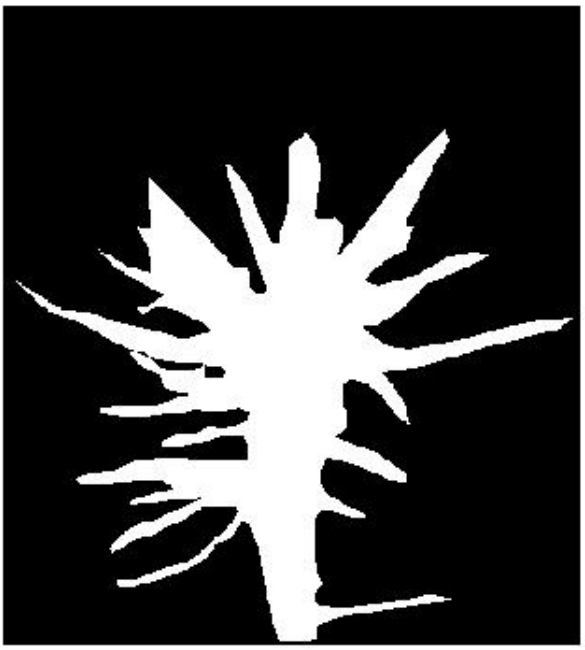

Figure 3: An example of ground truth

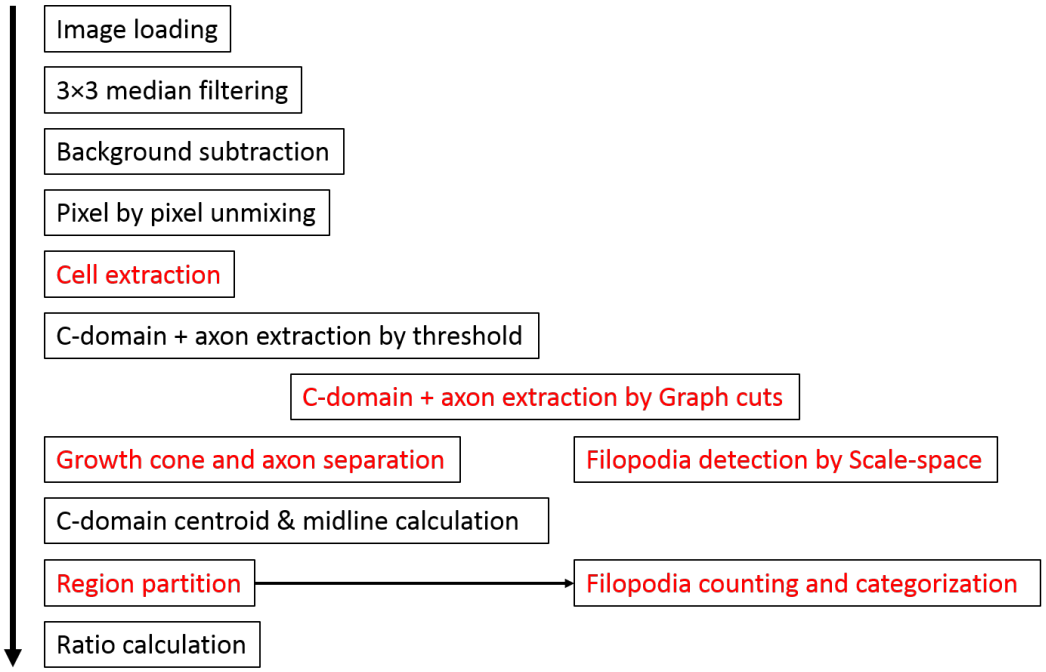

Figure 4: Flow of image proccesing

possible to segment a picture faster, however, since accuracy is more important in this program, Graph cuts method was chosen.

4.2.1 Graph cuts theory [4]

This theory can be used to segment a noisy image into two parts. In this thesis this is used to segment fore- and background. Then low cost cuts that cut connections between pixels are calculated by the Max-flow min-cut algorithm and where the cuts are considered as the boundary of two separated segments. The method combines information about individual pixel intensities as well as constraints on pairs of neighboring pixels.

Imagine that you want to segment an image like Figure 5 where the gray pixels are the foreground (cell in this thesis) and white are the background. The image is modeled as a graph, where every pixel is connected (edges) to surrounding 4 pixels and each pixel corresponds to a node. The weights of these edges are a constant 0.2, lambda. Using a higher weight will promote large connected segments. In Figure 6, there are 2 extra nodes, T and S. T represents background and S is foreground. Each edge connected to fore- and background has different weight. The weight of edge is set in such a way that if they are similar in intensity, the weight is high, and thus the min-cut results in foreground/background segmentation. The min-cut algorithm finds the cut that minimizes the sum of the weights between the pixels and the weights between the pixels and the S and T nodes.

One statistical approach is to think of this in probabilistic terms. If the

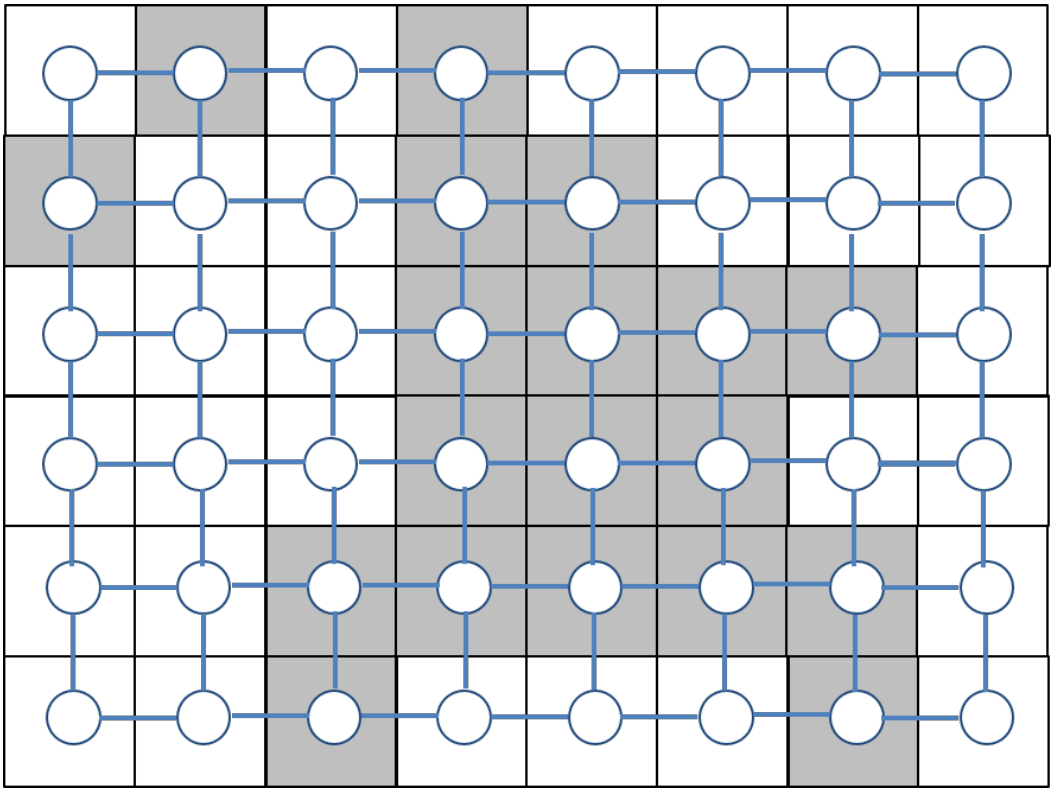

Figure 5: Example of graph correspond to an image

intensity of the foreground pixel can be modeled as a normal distribution, the probability of measuring an intensity x at a foreground pixel is

$$P(x \,|\, (\mu_{fg}, \sigma_{fg})) = N((\mu_{fg}, \sigma_{fg})) = \frac{1}{\sqrt{2\pi\sigma_{fg}^2}} \mathrm{e}^{-\frac{(x-\mu_{fg})^2}{2\sigma^2}} \quad .$$

Maximizing P is equal to minimizing $-log(P)$, which is proportional to

$$(x - \mu_{fg})^2 \quad .$$

This simplification is possible because the other parts in P are constant. Thus, in the program only the right part of this equation is calculated to estimate the edge weight between the pixel node and s/t node (Figure 7). The weights between the pixels can be viewed as putting a Markov Random Field prior on the foreground/background shapes.

4.2.2 Scale-space method [2]

This theory is used for edge detection. After applying Gaussian filter (Figure 8) and taking the local maxima, the intensity, first and second derivations of intensity were obtained. By comparing these values the edges are detected.

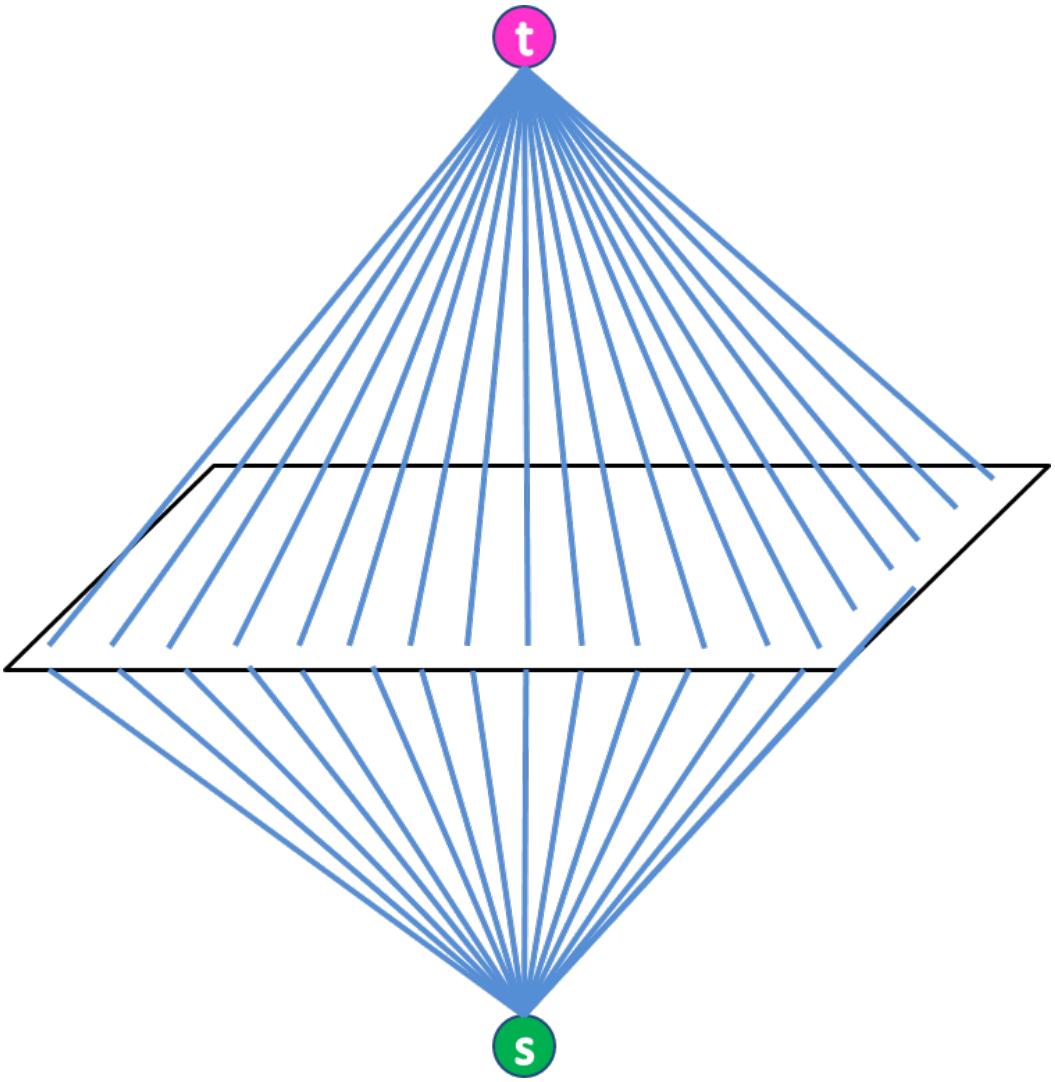

Figure 6: Image with s/t nodes and their weights shown as blue connection

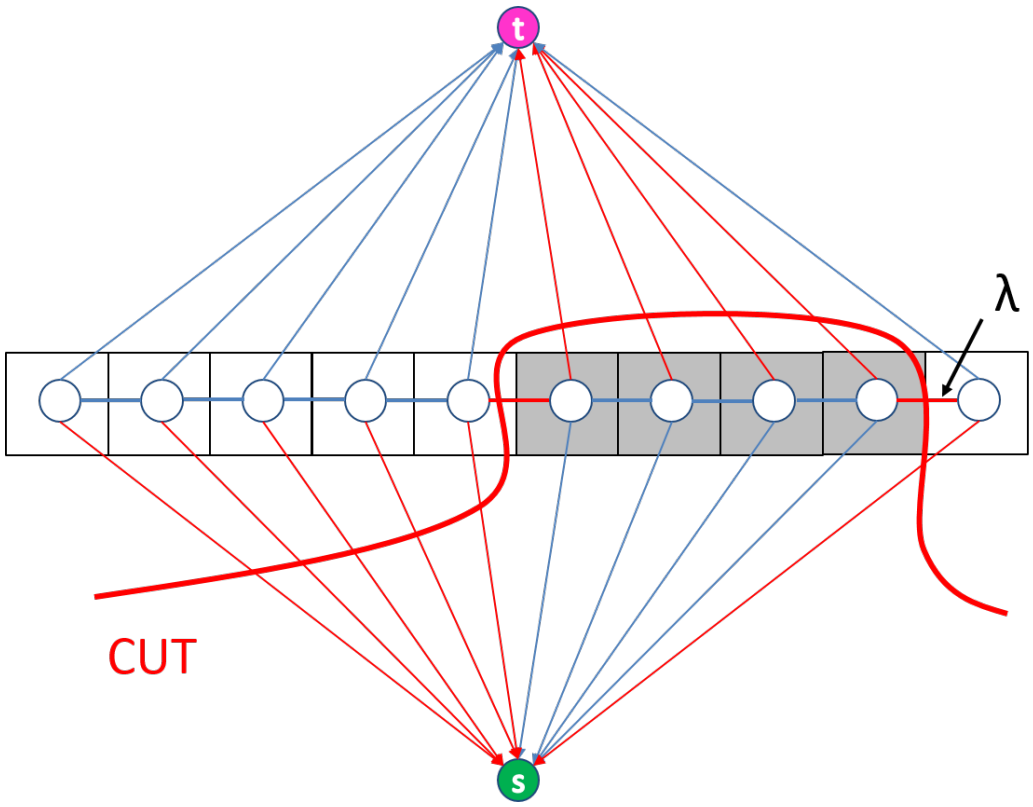

Figure 7: An example of min-cut of graph cuts

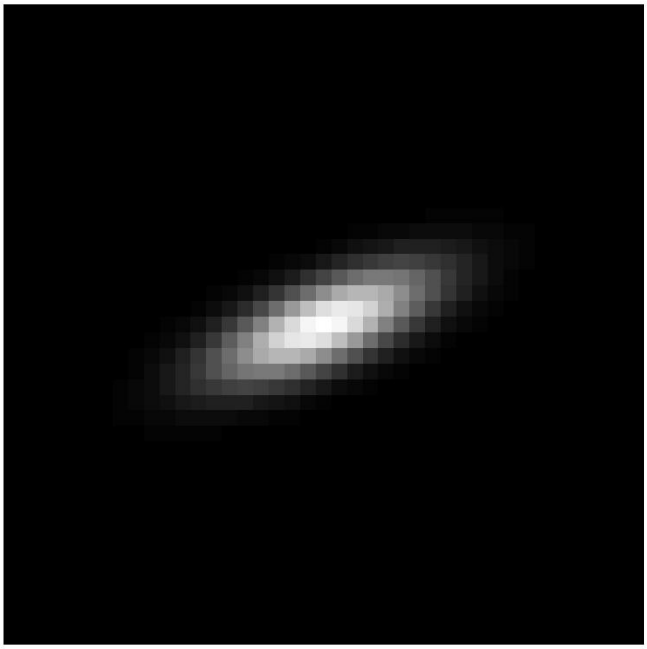

Figure 8: An elongated Gaussian filter

To optimize the Gaussian filter and take the local maxima, Newton-Raphson's Method was used to find next approximations. Finding the zero to a non-linear function f using the method is based on the linearization of the function f around the current estimate x_0, i.e.

$$f(x_0 + \Delta x) \approx f(x_0) + f'(x_0)\Delta x$$

By setting $f(x_0 + \Delta x) = 0$ we obtain $f(x_0) + f'(x_0)\Delta x = 0$ or

$$\Delta x = -\frac{f(x_0)}{f'(x_0)} \ .$$

Thus, the update is $x_{k+1} = x_k - f(x_k)/f'(x_k)$. This process is repeated until a sufficiently accurate value was reached.

4.3 Detailed Image processing

For the analysis of the growth cone and the axon, the acquired images were smoothed using a 3×3 median filter to reduce noise and the background was subtracted. For the filopodium counting, the original images are used. To obtain real fluorescence signal of each fluorescent protein, an unmixing process was applied to the fluorescence signals averaged within the ROIs according to

[3]. Finally, the FRET signals were calculated from the unmixed fluorescence pixel-by-pixel.

4.3.1 Cell (Growth cone + axon) extraction by threshold

The cell was first detected by thresholding by a semi auto process. By changing threshold manually a time laps with threshold boundary was shown in the images.

4.3.2 C-domain + axon separation by threshold

The C-domain + axon was first detected by thresholding by semi auto process. By changing threshold manually a time laps with threshold boundary was shown in the images. If there are some areas which is lower than threshold although they are inside C-domain + axon, they are considered higher than threshold.

4.3.3 C-domain separation by graph cuts

As well as the C-domain detection by thresholding, segmentation using the graph cuts method are used. Average of intensity in C-domain by threshold was used as foreground and the same average background taken by ROI in threshold method was used for background. The cut were calculated by Max-flow min-cut theorem according to the weights defined as described in background.

4.3.4 Axon separation

C-domain separated by graph cuts are used to estimate the boundary between axon and Growth cone. The boundary is, then, defined as at least 1σ wider in normal distribution when it is compared to the bottom of axon, which is thinnest in axon. There is also an option to input the boundary manually. To analyze the angles of growth cones the midline of the growth cones were calculated. It is defined as a line that links the centroid of C-domain and the center of the growth cone side terminal of axon. By calculating this line, angles of growth cone along images are estimated. Right half from above was shown as plus degree and left half was minus.

4.3.5 Filopodium detection

The filopodium were detected by scale-space method. First, C-domain + axon segmented by graph cuts is enlarged around 3 pixels from C-domain to avoid wrong filopodia. Then, ridges were detected for 16 different directions with convolution with an elongated Gaussian filter (Figure 8) at each pixel. After removing points detected inside growth cone and axon, local maxima were selected at each ridge and the directions were also calculated. Additionally, really small ridges (original Intensity without derivation is less than 0.04 and second derivation is less than 0.01) were removed and then optimization and clustering were carried out. The pixels that distance was less than 3 pixels and distance between interruption of perpendicular line to the other pixels' vector and the other pixel was less than 0.5 pixels, vice versa, were considered as a cluster (Figure 9). Too small clusters that had less than 40 components were considered

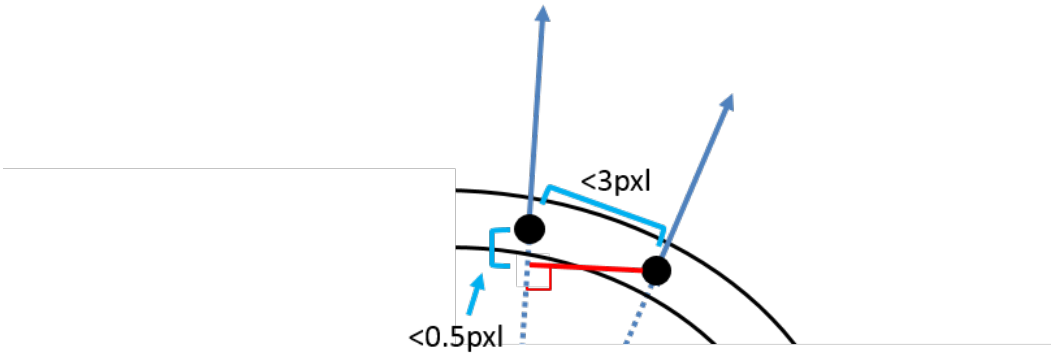

Figure 9: criteria and calculation of clustering

as noises and removed. Newton-Raphson's Method was applied to estimate optimized next positions. After all of these selections and calculations, clustered filopodia were detected.

Then filopodia are categorized into four different sections that are separated by the midline of growth cone and perpendicular line that interrupts at the centroid of C-domain. In the case a filopodium cluster lies across two sections it was categorized in the section which tip closer to C-domain belongs. Each direction of filopodium corresponding midline was also calculated.

5 Result

5.1 Cell segmentation

First of all, cell segmentation was carried out to obtain whole cell shape. Figure 10 shows cell detected by threshold and the green ridge show the boundary between background and cell. C-domain + Axon detection by threshold outputted similar images as well.

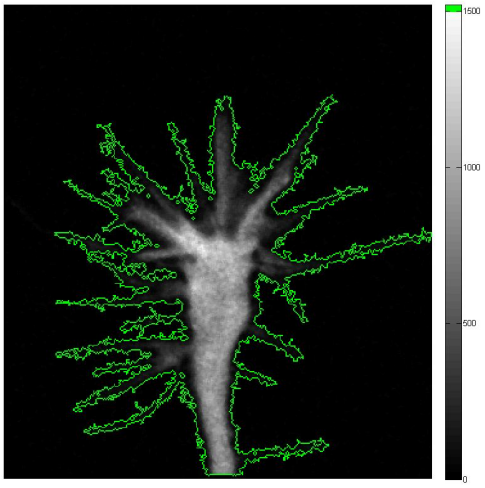

Figure 10: Image of cell segmentation

5.2 Evaluation of threshold method of cell segmentation

Figure 11 shows the comparison of threshold and ground truth in different time in time laps. The accuracy is measured by the intersection/union of threshold and grand truth, i.e.

$$\frac{\#(X_{thereshold}) \wedge (X_{groundtruth})}{\#(X_{thereshold}) \vee (X_{groundtruth})} \ . \tag{1}$$

This is the so called Jaccard index, see [7]. The average is $64.8 \pm 4.2\%$.

5.3 C-domain + Axon detection

Figure 12 is the C-domain + Axon area segmented by threshold and Figure 13 shows the segmented result by graph cuts.

5.4 Evaluation of Graph cuts method

Figure 14 shows the comparison of threshold and graph cuts in different time in time laps. The accuracy is measured by the Jaccard index. The average is $74.1 \pm 6.1\%$.

5.5 Growth cone and Axon separation

Separation of growth cone and axon depends on where the neck positions are. Figure 15 shows neck positions decided by two independent ways. The red dot represents neck position decided by new automatic way, while blue dot shows result of previous manual method. The average of mismatch of 10 time laps images were 3.5 ± 1.7 pixels.

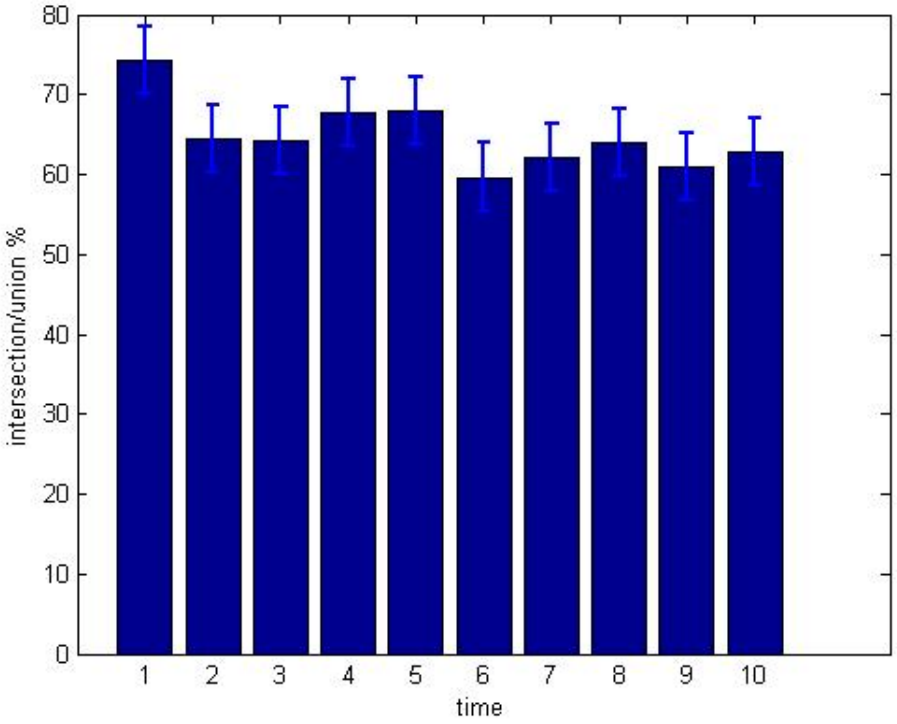

Figure 11: Comparison of threshold and ground truth

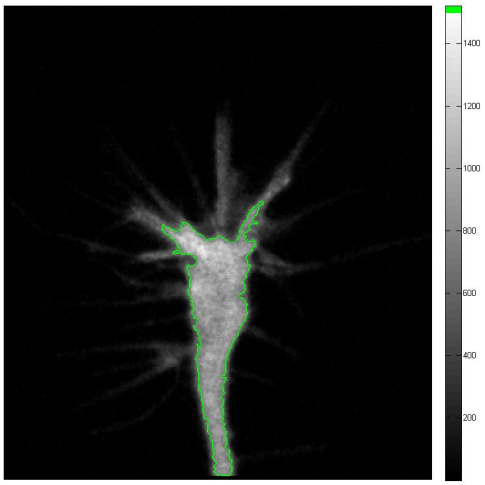

Figure 12: C-domain + Axon area segmented by threshold

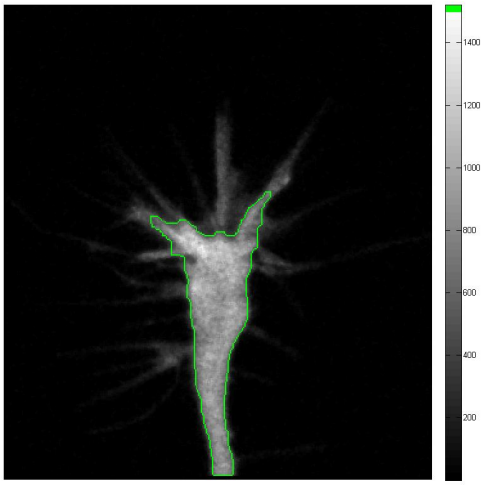

Figure 13: C-domain + Axon area segmented by graph cuts

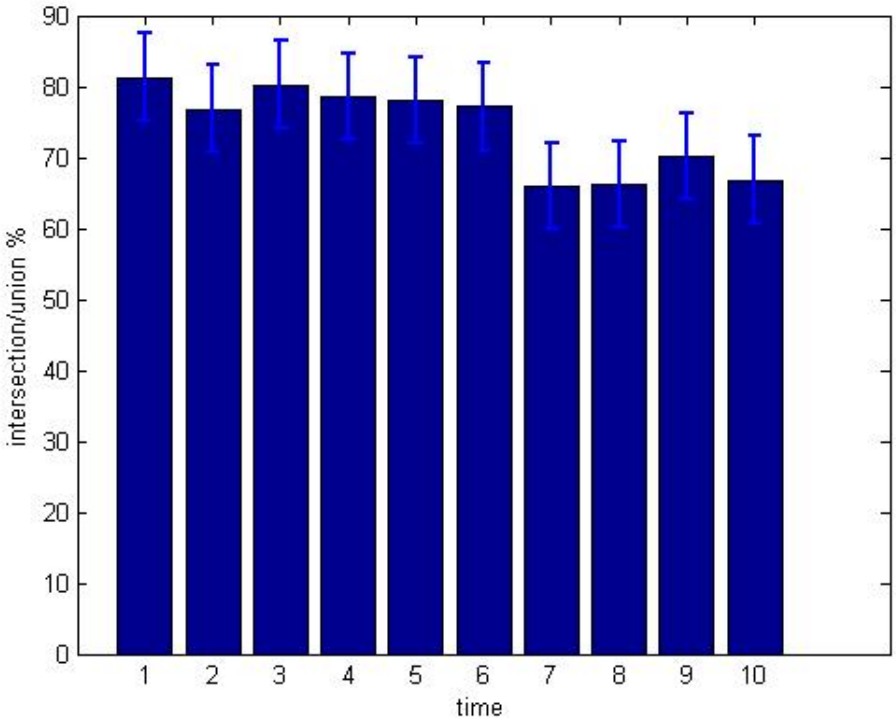

Figure 14: Comparison of threshold and graph cuts

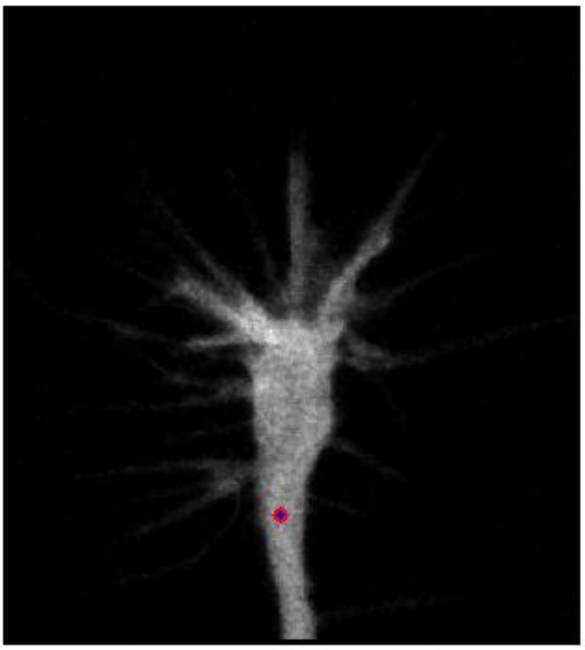

Figure 15: Neck positions by gragh cuts and ground truth

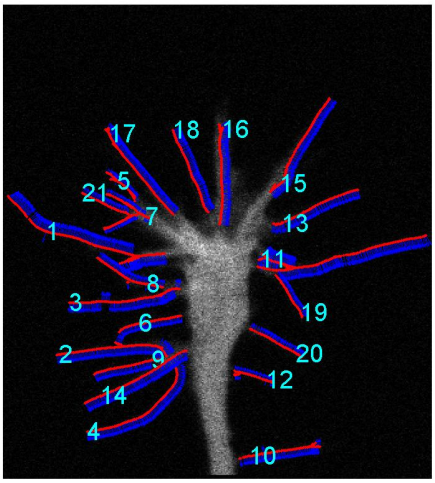

Figure 16: Detected filopodium

5.6 Filopodium detection

Filopodia were detected and counted (Figure 16). There are 21 filopodia in this image.

5.7 Filopodium slant calculation

Filopodium slants according to the midline are shown in Table 5.7 where midline is 0 degree and right half is plus. Furthermore, the extraction of slants is shown inFigure 17. partition shows that partition each filopodium belongs (Figure 18).

Table 1: Slant of dilopodium

No.	1	2	3	4	5	6	7	8	9	10	
partition	2	1	1	1	2	1	2	1	1	4	
degree	-72,8	-92,1	-100,0	-125,6	-47,5	-108,0	-105,9	-68,7	-104,3	78,7	
No.	11	12	13	14	15	16	17	18	19	20	21
partition	3	4	3	1	3	3	2	2	3	4	2
degree	76,5	102,2	65,4	-120,2	29,7	-3,3	-39,9	-26,2	144,9	116,1	-68,8

5.8 Region partition

Figure 18 shows categorized filopodia. The red dot in the middle represent C-domain centroid and the lines are midline and perpendicular line. Figure 18 Parted growth cone image

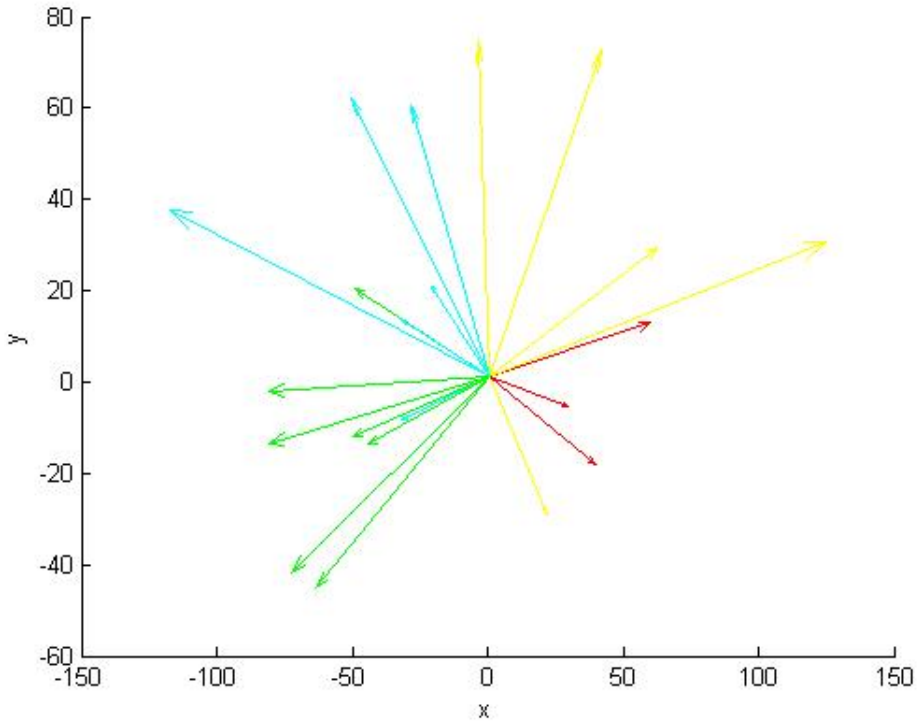

Figure 17: Slant of filopodia

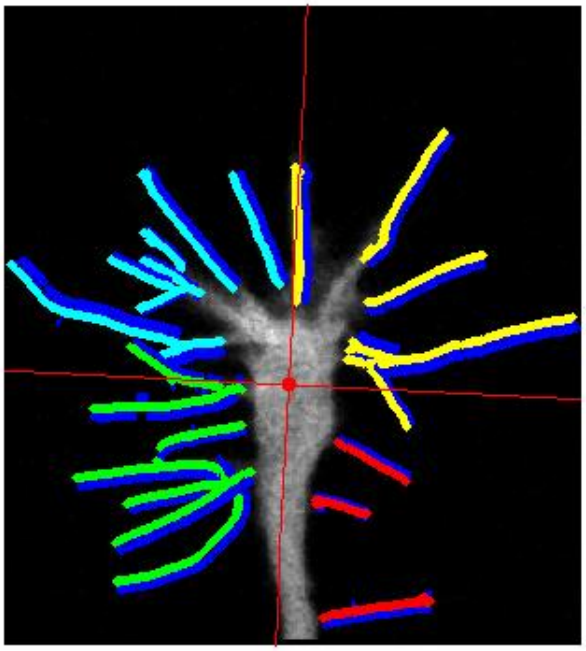

Figure 18: Parted growth cone image

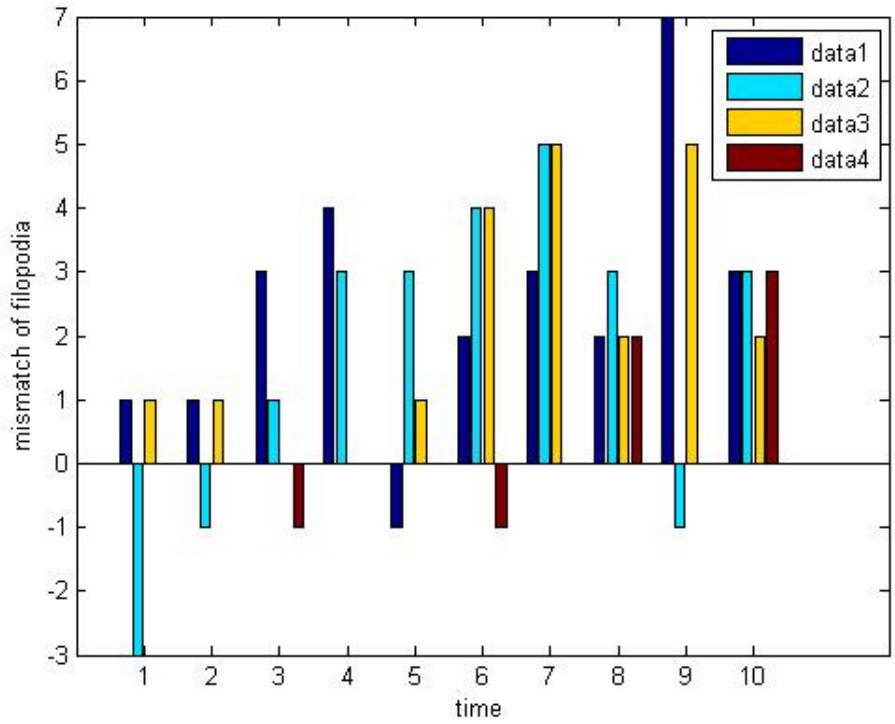

Figure 19: Comparison of number of filopodium detected in each partition

5.9 Evaluation of partition and filopodium counting

Table 5.9 shows numbers of filopodia determined in different partition by program. Figure 19 shows the comparison of filopodia detected by the program and manual counting. These are time laps images from time 1 to 10. As easily read from this graph at the beginning the mismatches are not obvious, however, after time 5 there are about 10 mismatches for each time. Data1-4 correspond the partition in Figure 18 clockwise from left bottom.

Table 2: Number of filopodium in each partition determined by program

		time									
		1	2	3	4	5	6	7	8	9	10
partition	1	7	6	9	10	5	8	8	8	13	9
	2	6	4	6	8	8	9	9	9	5	9
	3	5	5	5	4	6	7	8	7	10	9
	4	3	3	2	3	3	2	3	5	3	6

6 Discussion

6.1 Graph cuts methods

The C-domain detection using graph cuts works really well and it gives us a similar but smoother output if it is compared to the result of threshold. The result of graph cuts is used to segment axon and C-domain since it is smooth, while the result of threshold was too noisy and could not be processed. Comparing the result with the comparison between ground truth and threshold, it is more similar to threshold method. In conclusion, this method works well to separate the part where we wanted.

6.2 Axon and Growth cone separation

The results shown in the result are really ideal and the mismatch between two different methods is really small. However it is a question if this result is reliable because there are some different definitions of axon and growth cone, thus it is difficult to decide an identical position just from shape of growth cone. Since this cannot be clearly solved we need to double-check each time, whether the position is settled properly.

6.3 Filopodia counting by scale-space method

It seems that this software could detect filopodia accurately on the result. There are, however, some weaknesses we could find from the results. When there are many lamellipodia (flat layer between filopodia) this program detects too many filopodia there (Figure 20, Figure 21). We could tune the parameters used in this program or also as an option we could try to use another method instead of Scale-space method.

6.4 For further work

This software worked well in this set of images. There are, however, some improvements we need to achieve in the future.

1. Further development of program is required. This program output suitable result when the images are clear enough and since taking a clear images of growth cone is quit hard, thus it will be really helpful if we can develop a program to analyze noisier images as well as clear images. Moreover it will need to be adjusted to growth cone out growth and a variety of growth cone shapes.

2. Extract information from shape and reveal the relation between chemical signals and different structure or movement. Now as the first tool is established, we need to think how we can exploit the results of this program. One idea is to calculate information entropy of growth cone and compare at different phases.

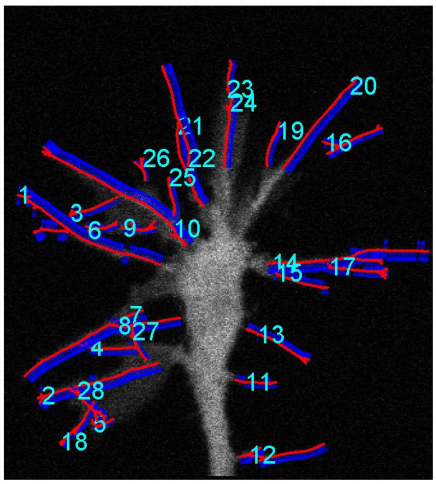

Figure 20: Detected pseudo filopodia (number)

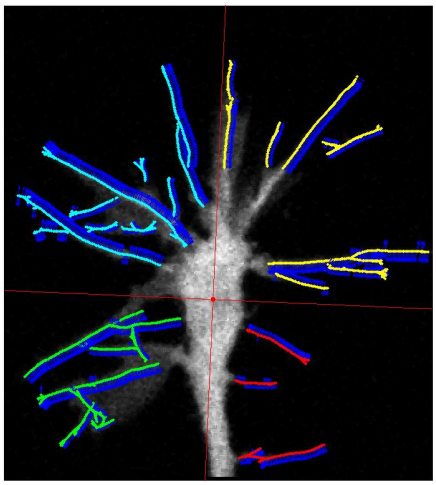

Figure 21: Detected pseudo filopodia (Partition)

7 Conclusions

With this software, listed things were achieved.
-Development of segmentation by graph cuts method
-Evaluation of threshold and graph cuts methods
-Development of filopodia counting program
-Development of filopodia categorizing program
-Development of filopodia slant calculation
-Evaluation of filopodia counting

Acknowledgements

I would like to express my special appreciation and thanks to my supervisor Prof. Kalle Åström. It was the happiest day during my study in Lund University when he accepted me as a master thesis student. His advices on both research and career were precious for me.

I would like to thank my supervisor Prof. Kotaro Oka for his many advices on my thesis. From some discussions via skype I learned many ideas for my research.

I would like to thank a Ph.D student Fangyuan Jiang for his technical support and advices on my thesis. Without his supports I would not be able to complete this work.

I would like to thank Prof. Anders Heyden and Associate Prof. Stefan Diehl for his advices and brilliant comments especially on the presentation.

I also would like to appreciate Prof. Olle Holst at Biotechnology department. He organized whole my master study in Lund and supported my thesis.

I would like to thank all staffs in Lund, friends at biotechnology department and the other, and other people who supported my in Lund.

A special thanks to my family, especially to my parents. I cannot express my gratitude for supporting and thinking of me from Japan.

Thank you all again for those who made my life, study, time in Lund.

References

[1] Kobayashi, T., Nagase, F., Hotta, K. , Oka, K. Crosstalk between Second Messengers Predicts the Motility of the Growth Cone. Sci. Rep. 3, 3118; DOI:10.1038/srep03118 (2013).

[2] Åström, K. Heyden, A.. Stochastic Analysis of Image Acquisition, Interpolation and Scale-space Smoothing, Adv. Appl. Prob. (SGSA) **31**, 855-894 (1999).

[3] Niino, Y., Hotta, K. , Oka, K. Simultaneous live cell imaging using dual FRET sensors with a single excitation light. PloS one 4, e6036 (2009).

[4] Yuri B., Olga V., Ramin Z., Fast Aproximate Energy Minimization via Graph Cuts, IEEE transactions on Pattern Analysis and Machine Intelligence,**23**, 11, 1222–1239 (2001).

[5] Laura Anne Lowery, David Van Vactor, The trip of the tip: understanding the growth cone machinery, Nature Reviews Molecular Cell Biology 10, 332-343 (May 2009).

[6] Björn Nilsson, Anders Heyden. A fast algorithm for level set-like active contours, Pattern Recognition Letters **24**, 1331-1337 (2003).

[7] Jaccard, Paul "tude comparative de la distribution florale dans une portion des Alpes et des Jura", Bulletin de la Socit Vaudoise des Sciences Naturelles 37: 547579 (1901).

Master's Theses in Mathematical Sciences 2013:E67
ISSN 1404-6342

LUTFMA-3256-2013

Mathematics
Centre for Mathematical Sciences
Lund University
Box 118, SE-221 00 Lund, Sweden

http://www.maths.lth.se/